DETERMINATION OF THE DISTANCE TO M33 BASED ON THE TIP OF THE RED GIANT BRANCH AND THE RED CLUMP[1]

Minsun Kim, Eunhyeuk Kim, Myung Gyoon Lee
Astronomy Program, SEES, Seoul National University, Seoul, 151-742, Korea
Ata Sarajedini
Department of Astronomy, University of Florida, P.O.Box 112055, Gainsville, FL 32611, USA
Doug Geisler
Departamento de Física, Grupo de Astronomía, Universidad de Concepción, Casilla 160-C, Concepción, Chile
Draft version October 2, 2001

ABSTRACT

We have determined the distance to M33 using the tip of the red giant branch (TRGB) and the red clump (RC), from the VI photometry of stars in ten regions of M33 based on $HST/WFPC2$ images. The regions used in this study are located at $R = 2.6 - 17.8$ arcmin from the center of M33. The distance modulus to M33 obtained in this study, for an adopted foreground reddening of $E(B-V) = 0.04$, is $(m-M)_{0,TRGB} = 24.81 \pm 0.04(\mathrm{random})^{+0.15}_{-0.11}(\mathrm{systematic})$ from the TRGB, and $(m-M)_{0,RC} = 24.80 \pm 0.04(\mathrm{random}) \pm 0.05(\mathrm{systematic})$ from the RC, showing an excellent agreement between the two (corresponding to a distance of 916 ± 17(random) kpc and 912 ± 17(random) kpc, respectively). These results are ≈ 0.3 mag larger than the Cepheid distances based on the same $HST/WFPC2$ data and ground-based data. This difference is considered partially due to the uncertainty in the estimates of the total reddening for Cepheids in M33.

Subject headings: galaxies: distances and redshifts — galaxies: individual (M33 (NGC 598)) — stars: tip of the red giant branch (TRGB) — stars: red clump(RC)

1. INTRODUCTION

The accurate determination of the distances to Local Group galaxies is critical in the study of the extragalactic distance scale. In particular two spiral galaxies in the Local Group, M31 and M33, are primary calibrators for several secondary distance indicators including the Tully-Fisher relation. While the distance to M31 has been measured extensively, relatively less attention has been paid to the distance determination of M33 (van den Bergh 2000).

Recently the tip of the red giant branch (TRGB), a Population II distance indicator, has frequently been used for the determination of distances to resolved galaxies in the Local Group; in addition, another Population II distance indicator, the red clump (RC), has come to be used quite often as well. These two methods have an advantage over the classical primary distance indicators such as Cepheids and RR Lyraes in that the distances to galaxies can be determined reliably from single epoch observations. The TRGB has been known to be an excellent standard candle for resolved galaxies, because the I-band magnitude of the TRGB for stars older than a few Gyrs with metallicity $-2.1 \leq [Fe/H] \leq -0.7$ is essentially independent of age and metallicity (Lee, Freedman, & Madore 1993; Lee 1996; Salaris & Cassisi 1998; Ferrarese et al. 2000; Cioni et al. 2000).

On the other hand, the RC was not widely recognized as a potentially good standard candle until Paczyński & Stanek (1998) recently suggested its use. Since then the reliability of the RC as a standard candle has been controversial (see Sarajedini (1999); Girardi & Salaris (2001); Popowski (2000) and the references therein). Paczyński & Stanek (1998) showed that the mean I-band magnitude M_I^{RC} of red clump stars is independent of their color in the range $0.8 \leq (V-I)_0 \leq 1.4$ and has a small dispersion(≈ 0.2 mag), suggesting that the RC can be a good standard candle as originally pointed out by Cannon (1970). However, the distance to the Large Magellanic Cloud obtained using the RC by Stanek, Zaritsky, & Harris (1998) and Udalski et al. (1998) was much shorter than that based on other methods, which became a starting point for debate focused on the accuracy of the RC method. Udalski (1998) claimed that the M_I^{RC} has a weak dependence on metallicity and no dependence on age for an intermediate age population (2–10 Gyrs) of stars. On the contrary, Sarajedini (1999) analyzed several galactic open clusters with intermediate-ages and compared the properties of their RCs with the predictions of stellar evolution models; this comparison indicates that the M_I^{RC} becomes significantly fainter as the cluster gets older. In addition, a number of studies have argued that stellar evolutionary theory predicts a significant dependence of M_I^{RC} on the combination of the age and metallicity of the stellar population (Cole 1998; Girardi et al. 1998; Girardi 2000; Girardi & Salaris 2001). Castellani et al. (2000) pointed out that the input physics and the dependence of various evolutionary codes should be considered to clarify this discrepancy. Observationally it is also important to attack this problem by investigating the effect of age and metallicity on the RC in other nearby galaxies where the properties of the RC can be studied in detail.

In this paper we present an analysis designed to determine the distance to M33 using the TRGB and the RC based on photometry of stars in ten M33 fields obtained

[1] Based on observations with the NASA/ESA Hubble Space Telescope obtained at the Space Telescope Science Institute, which is operated by the Association of Universities for Research in Astronomy, Incorporated, under NASA contract NAS5-26555.

from $HST/WFPC2$ images. M33 is an ideal target to apply both the TRGB and RC methods of distance determination using $HST/WFPC2$ data.

This paper is composed as follows. In §2 we present the data and reduction technique. §3 displays the color-magnitude diagrams of the measured stars, and estimates the distance to M33 using the TRGB and RC methods. Primary results are discussed in §4 and are summarized in §5.

2. DATA AND REDUCTION

We have analyzed $HST/WFPC2$ data for ten fields in M33 obtained for Sarajedini et al. (1998)'s cycle 5 program (GO-5914). Each field was observed for four orbits, yielding a total exposure time of 4800 seconds for $F555W(V)$ and 5200 seconds for $F814W(I)$. These data were obtained originally for the study of globular clusters in M33, and a globular cluster is centered in each PC chip. The data from the PC chip were presented by Sarajedini et al. (1998) and Sarajedini et al. (2000). In this study we use all field stars in the WF2, WF3, and WF4 chips as well as in the PC chip. Hereafter we refer to each observed region using the globular cluster's designation. Figure 1 illustrates the location of the regions in M33 used in this study. Considering the number of fields and the deep exposures, these data are ideal for studying the field stars as well as the globular clusters in M33.

Table 1 lists the positions, galactocentric distances, deprojected radial distances, and the reddening values of all the regions used in this study. The position of the region in Table 1 is the center of the WFPC2. The galactocentric distance is the distance from the center of M33 (RA(2000) = $01^h33^m51^s.02$, Dec(2000) =$+30°39'36''.7$) (Cotton, Condon, & Arbizzani 1999). All the regions were assumed to be in the plane of M33's disk and were deprojected to estimate the actual radial distance. An inclination of 56° and a position angle of 23° for M33 were used for deprojection of the positions (Regan & Vogel 1994). For foreground reddening correction, the COBE/IRAS extinction maps of Schlegel, Finkbeiner, & Davis (1998) are used. The reddening values of all the regions are as low as $E(V-I) = 0.06$ ($E(B-V) = 0.04$). The extinction laws for R_V =3.3, $A_I = 1.95E(B-V)$ and $E(V-I) = 1.35E(B-V)$ (Cardelli et al. 1989), are adopted in this study.

The photometry of the stars in the CCD images has been obtained using the *multiphot* routine of the HSTphot package (Dolphin 2000a). The HSTphot package was designed for photometry of $HST/WFPC2$ data and employs a library of Tiny Tim point-spread-functions (PSFs) for PSF fitting to account for variations in the PSF due to location on the chip and the centering within a pixel. After PSF-fitting, corrections are also made for geometric distortion, CTE effect, and the 34^{th} row effect (Dolphin 2000b). The *multiphot* routine gives the magnitudes transformed to the standard system as well as instrumental magnitudes. The HSTphot photometry used zero points from Dolphin (2000b) which provides corrections to the Holtzman et al. (1995) values.

3. RESULTS

3.1. *Color-Magnitude Diagrams*

The number of the measured stars in each region is many tens of thousands (from $\sim$ 60000 to $\sim$ 80000 stars) which are too many to plot in a color-magnitude diagram (CMD). Therefore, as an example, Fig. 2 shows the color-magnitude diagram (CMD) for one field. In the case of the PC chip, at the center of which a globular cluster is located, the stars at $r < 2.8$ arcsec from the center of the cluster are considered to be members while those at $r > 4.6$ arcsec are considered to be field stars. Figure 2 shows a CMD for the measured stars in the C20-region, which happens to be our most distant field from the center of M33. Several features are seen in Figure 2. (a) There is a broad red giant branch (RGB), the tip of which is seen at $I \approx 21.0$ mag. The mean color of the RGB of these field stars is redder than that of the globular cluster C20 in the same region (represented by the solid line). The locus of C20 was derived from the median color of the stars at $r < 2.8$ arcsec from the center of C20. (b) A red clump is distinctively seen at $I \approx 24.5$ mag and $(V-I) \approx 1.0$; (c) Asymptotic giant branch (AGB) stars are also seen along and above the RGB; and (d) There is a blue plume at $(V-I) \approx 0.0$ extending up to $I \approx 20$ mag, which consists of massive main sequence stars and evolved supergiants. These features are also seen in the CMDs of the other regions.

In Figure 3, the CMDs of all the regions are shown in number density contour maps (Hess Diagrams). The density contour maps are constructed on 100×100 grids in the CMD domain (the size of each grid is $\Delta(V-I) \times \Delta I = 0.03 \times 0.1$), and are smoothed using Gaussian filters of 2 grid width. Basic features seen in Figure 3 are similar to those in Figure 2. Number density contour maps are useful for revealing the areas with the highest stellar density. All CMDs in Figure 3 show a strong peak at the position of the red clump (marked by the crosses). The photometry of the stars in the R14- and R12-regions is significantly affected by crowding, because they are located close to the center of M33. Therefore only the stars in the PC chip (which has higher spatial resolution than the WF chips) are used to measure the magnitude of the red clump in these regions in the following.

3.2. *Estimation of the Distance to M33*

3.2.1. *Tip of the Red Giant Branch*

We have determined the distance to M33 using the I-band magnitude of the TRGB, following the description given in Lee, Freedman, & Madore (1993). Figure 4 displays the I-band luminosity functions of red stars including the RGB and AGB stars. In Figure 4 there is a sudden increase at $I_{TRGB} \approx 20.9$ in all the regions as marked by the arrow, which corresponds to the TRGB. We have measured the I-band magnitude of the TRGB using this feature in the luminosity function by eye detection (supplemented by using the edge-detection filters (Lee, Freedman, & Madore 1993)). The values of the I_{TRGB} thus derived for all the regions are listed in Table 2.

The distance modulus is given by

$$(m-M)_I = I_{0,TRGB} + BC_I - M_{bol,TRGB} \qquad (1)$$

where $I_{0,TRGB}$ is the dereddened I-band magnitude of the TRGB. BC_I is the bolometric correction to the I magni-

tude which depends on color as follows:

$$BC_I = 0.881 - 0.243(V-I)_{0,TRGB} \quad (2)$$

where $(V-I)_{0,TRGB}$ is the dereddened color of the TRGB.

The bolometric magnitude of the TRGB, $M_{bol,TRGB}$, is given as a function of metallicity [Fe/H] by:

$$M_{bol,TRGB} = -0.19[Fe/H] - 3.81. \quad (3)$$

Metallicity can be estimated from the $(V-I)$ color at the absolute I-band magnitude of $M_I = -3.5$ given by Lee, Freedman, & Madore (1993) (see also Saviane et al. (2000)) as follows:

$$[Fe/H] = -12.64 + 12.6(V-I)_{0,-3.5} - 3.3(V-I)^2_{0,-3.5}. \quad (4)$$

We have employed an iterative procedure in which an initial guess at the distance is used to estimate the metallicity which is in turn used to refine the distance until the solution converges, which occurs after only a few iterations. It is important to note that the regions used for this study are located in various environments including young to old stellar populations; thus, the broad RGBs seen in the CMDs are actually a mixture of intermediate-age to old populations, as well as a range of metallicities. If we simply use the mean color $[(V-I)_{0,-3.5}]$ of the entire apparent RGB in this case, the resulting metallicity will be an underestimate, because there are younger populations with bluer color on the blue side of the RGB. For this reason we tried to use the median value of the color of the stars along the RGB to reduce the effect of intermediate-age populations. As a check of our method, we have also derived the mean metallicity using the slope of the RGB as calibrated by Sarajedini et al. (2000), obtaining very similar results to those from the median color of the RGB stars.

The mean metallicities resulting from this procedure are listed in Table 2. The mean metallicity ranges from [Fe/H] $\approx$ –0.6 to –0.9 dex. Figure 5 displays the mean metallicity versus the deprojected radial distance of the regions (filled circles). In Figure 5 there is clearly a negative radial gradient of the metallicity. The mean metallicity data are fit by [Fe/H] $= -0.05[\pm0.01]R_{dp} - 0.55[\pm0.02]$ ([Fe/H] $= -0.04[\pm0.02]R_{dp} - 0.51[\pm0.06]$, using the metallicity obtained with the RGB slope method) for all the data, where R_{dp} is given in terms of kpc ($1' = 0.27$ kpc is assumed). If we exclude the two innermost regions where the crowding is severe, we obtain a fit, [Fe/H] $= -0.07[\pm0.01]R_{dp} - 0.48[\pm0.04]$ ([Fe/H] $= -0.08[\pm0.03]R_{dp} - 0.34[\pm0.10]$ using the metallicity obtained with the RGB slope method), similar to values found in our Galaxy's disk using open clusters and field giants ($d[Fe/H]/dR = -0.050 \pm 0.008$ kpc^{-1}) (Janes 1979).

In Figure 5 the metallicity of the red giants is compared with that of HII regions in M33. The metallicity of the HII regions was converted from [O/H] values given in the literature (Kwitter & Aller 1981; McCall, Rybski, & Shields 1985; Vilchez et al. 1988; Zaritsky, Kennicutt, & Huchra 1994) using the following relation taken from King (2000): $[O/Fe] = -0.184[Fe/H] + 0.019$. The deprojected radius for the HII regions was calculated as above. The metallicity of the HII regions is fit by [Fe/H] $= -0.12[\pm0.02]R_{dp} + 0.33[\pm0.07]$, which is somewhat steeper than that for the field red giants. The relation for the HII regions shows a trend that is similar to that of the field red giants, but with a larger scatter. It is natural that the mean metallicity of the field red giants is lower than that of the HII regions, because the red giants are much older than the HII regions.

Then we derive the distance modulus of each region using the information given above. Table 2 lists the parameters related to the TRGB method; the observed I-band magnitude of the TRGB (I_{TRGB}), the extinction corrected I-band magnitude of the TRGB ($I_{0,TRGB}$), the mean color of the TRGB $[(V-I)_{0,TRGB}]$, the mean color measured at $M_I = -3.5$ $[(V-I)_{0,-3.5}]$, the mean metallicity ([Fe/H]) of the RGB, the absolute magnitude of the TRGB ($M_{I,TRGB}$), and the distance modulus $[(m-M)_0]$.

Figure 6 displays I_{TRGB} versus [Fe/H] for the ten regions in M33. The value of I_{TRGB} varies little, with no obvious net metallicity dependence. The mean value of I_{TRGB} for the ten regions is $I_{TRGB} = 20.88 \pm 0.04$, showing a remarkably small dispersion.

The average value of the distance moduli for all of the fields is calculated to be $(m-M)_{0,TRGB} = 24.81 \pm 0.04(\text{random})^{+0.15}_{-0.11}(\text{systematic})$. The errors for the distance modulus are based on the error budget listed in Table 3.

The calibration of the TRGB is based on Galactic globular clusters with [Fe/H] = –2.1 to –0.7 dex, yet the derived mean metallicities of the four inner regions in our sample ([Fe/H] = –0.61 to –0.68 dex) are slightly larger than the upper boundary of the calibration range. If we use only the six other regions, excluding these four inner ones, we obtain an average distance modulus of $(m-M)_{0,TRGB} = 24.83 \pm 0.06(\text{random})^{+0.15}_{-0.11}(\text{systematic})$. If the theoretical calibration given by Salaris & Cassisi (1998) is adopted ($M_{I,TRGB} = -3.953 + 0.437[M/H] + 0.147[M/H]^2$ and $[M/H] = -39.270 + 64.687[(V-I)_{0,-3.5}] - 36.351[(V-I)_{0,-3.5}]^2 + 6.838[(V-I)_{0,-3.5}]^3$), the average distance modulus will be $(m-M)_{0,TRGB} = 24.99 \pm 0.04$(statistical), which is 0.2 mag fainter than that derived using the empirical calibration of Lee, Freedman, & Madore (1993). However, it has been found that the distance obtained with the theoretical calibration is not consistent with other results as shown by Dolphin et al. (2001) in IC 1613. So we prefer to use the empirical calibration rather than the theoretical one in this study. Finally we adopt $(m-M)_{0,TRGB} = 24.81 \pm 0.04(\text{random})^{+0.15}_{-0.11}(\text{systematic})$ as the TRGB distance modulus to M33.

3.2.2. *Red Clump Stars*

We have determined the distance to M33 using the red clump as well. Red clumps are clearly found in the CMDs of all the regions, as seen in Figure 3. It is important to note that implicit in the subsequent analysis is the assumption that the metallicity determined from the RGB stars can be applied to the red clump stars as well. This is based on two assertions. First, based on the absence of a vertical structure of stars blueward of the RC (Girardi & Salaris 2001), we claim that the age of the RC stars is likely to be older than ∼1 Gyr. Second, the chemical enrichment in the disk of M33 is assumed to have been small in the period between 10 Gyr and a few Gyr ago.

To check the variation of the mean magnitude of the red clump on the color, we have selected red clump stars with colors and magnitudes in the range $0.6 < (V-I) < 1.6$ and $23.5 < I < 25.5$. Figure 7 displays the mean magnitude of these stars (I_{RC}) versus their $(V-I)$ colors. The horizontal bars on the filled circles represent the size of the color bin. Two thousand stars are included in each color bin.

Figure 7 shows that the variation of the mean magnitudes for the color range of $0.8 \leq (V-I) \leq 1.2$ in a given region (the same range as used for M31 by Stanek & Garnavich (1998)) is smaller than 0.1 mag in all of the regions; Fig. 7 also indicates that the variation of the mean magnitudes among the regions is remarkably small (less than 0.1 mag). It is rather surprising that the variation of the mean magnitudes of the RC is smaller than 0.1 mag, considering that the regions used are located at a large range of distances from the center of M33 with diverse star formation histories and a varying metallicity. However, we note that the metal abundances vary over a range of less than 0.3 dex. Such a small abundance range has a correspondingly small effect on the I-band RC luminosity (less than 0.04 mag)(Girardi & Salaris 2001; Sarajedini 1999). The RC is also sensitive to age, which further suggests that the dominant stellar populations in our M33 disk fields are all probably similar in age. In uniform populations such as this, the red clump can potentially be a good standard candle.

We derive then the I-band luminosity functions of these red clump stars with $0.8 \leq (V-I) \leq 1.2$, as displayed in Figure 8. Figure 8 shows that there is a strong single peak above the slowly varying background in the I-band luminosity functions in all the regions. We measure the peak magnitude of the red clumps fitting the I-band luminosity functions with the combination of a gaussian function (for the red clump) and a parabolic function (for the red giants and subgiants) as follows (Paczyński & Stanek 1998):

$$N(I_{rc}) = a+b(I-I_{rc})+c(I-I_{rc})^2+\frac{N_{RC}}{\sigma_{RC}\sqrt{2\pi}}\exp\left[\frac{-(I-I_{rc})^2}{2\sigma_{RC}^2}\right]. \quad (5)$$

Figure 8 shows that the data for the I-band luminosity functions are well fit by the equations (the solid lines), and the fitting parameters thus derived are listed in Table 4. For the R14 and R12 regions in Figure 8, in which only the stars in the PC chip are used because of crowding, the luminosity functions are arbitrarily multiplied by a factor of 5 for plotting. Remarkably, the peak magnitudes of the red clumps of all the regions turn out to be within a very narrow range from $I_{RC} = 24.46$ to 24.57.

Then we need to know the absolute magnitude of the red clump to derive the distance modulus. Calibration of the absolute magnitude of the red clump is a matter of considerable debate (see Girardi & Salaris (2001) and references therein). As a result, the calibrations of the relation between the I-band magnitude and metallicity of the red clump continue to change. In fact, these relations should include the effects of age, but rarely do because of the difficulty in estimating the ages of individual field stars. Two of the most recent empirical calibrations are

$$M_I^{RC} = 0.19[\pm0.05][Fe/H] - 0.23[\pm0.03] \quad (6)$$

given by Popowski (2000) with the metallicity range of $-1.9 \leq [Fe/H] \leq 0.0$, and

$$M_I^{RC} = 0.13[\pm0.07][Fe/H] - 0.23[\pm0.02]. \quad (7)$$

given by Udalski (2000) with the metallicity range of $-0.6 \leq [Fe/H] \leq 0.05$.

Assuming that the mean metallicity of the red clump in all the regions in our study is similar to that of the red giants and that the eqs.(6) and (7) are universal, we derive the distance to M33 using the above calibrations. The results thus obtained are summarized in Table 4. Table 4 lists the estimated parameters related to the red clump method; the peak magnitude of the red clump (I_{RC}), the dereddened peak magnitude of the red clump ($I_{0,RC}$), the dispersion of the peak magnitude of the red clump (σ_{RC}), the mean color of the red clump $[(V-I)_{0,RC}]$, the metallicity ($[Fe/H]$) (from Table 2), the distance modulus from equation (6), and the distance modulus from equation (7).

We have investigated the relations between these parameters in Figure 9 wherein (a) illustrates the mean color of the red clump stars as a function of [Fe/H]. This figure shows that the mean color of the red clump is almost constant among the regions, with an average value, $(V-I)_{RC} = 0.98 \pm 0.02$ (represented by the dashed line).

Figure 9(b) displays σ_{RC} versus [Fe/H]. σ_{RC} is almost constant at 0.24 ± 0.02 for [Fe/H] < -0.7 dex, and increases significantly for [Fe/H] > -0.7 dex. This increase is mainly due to the crowding problem in the inner regions of M33 with [Fe/H] > -0.7 dex.

Figure 9(c) illustrates the extinction-corrected I-band magnitude of the red clump versus [Fe/H]. It is clear that the I-band magnitude of the red clump becomes fainter as [Fe/H] increases. The data for all the regions are fit well by $I_{0,RC} = 0.33[\pm0.10]$[Fe/H]$+24.67[\pm0.07]$ (leading to $M_{RC}^I = 0.33[\pm0.10]$[Fe/H]$-0.14[\pm0.07]$ when $(m-M)_0 = 24.81$ is adopted. If using only the outer 8 regions for the fit, the relations are $I_{0,RC} = 0.28[\pm0.14]$[Fe/H]$+24.63[\pm0.10]$ ($M_{RC}^I = 0.28[\pm0.14]$[Fe/H]$-0.18[\pm0.10]$ when $(m-M)_0 = 24.81$ is adopted). The slope in this fit is somewhat steeper than that of the calibration given by Popowski (2000), 0.19, (the dashed line). Noting that the result on the slope is based on the assumption that the metallicity of the RGB in M33 is the same as that of the RC, determination of the metallicity of the RC is needed to confirm it.

If we normalize the fitting result based on the outer 8 regions to the local Hipparcos red clump result of $M_{RC}^I = -0.23 \pm 0.02$ at $[Fe/H] = 0.0$ (Stanek & Garnavich 1998), then the relation between M_{RC}^I and $[Fe/H]$ is derived as follows.

$$M_I^{RC} = 0.28[\pm0.14]([Fe/H] - 0.18) - 0.18[\pm0.02]. \quad (8)$$

The distance modulus obtained using eq.(8) is $(m-M)_0 = 24.86 \pm 0.04$, which is slightly larger than the distance moduli based on Popowski (2000)'s and Udalski (2000)'s calibration of M_{RC}^I (see below).

As emphasized earlier, models predict that M_{RC}^I depends on metallicity and age (Cole 1998; Girardi et al. 1998; Girardi 2000; Girardi & Salaris 2001). The sensitivity to metal abundance is explicitly shown in Fig. 9(c) and quantified in the discussion above. The dependence

on age is likely to be manifested in the dispersion around the dotted line in Fig. 9(c). This dispersion amounts to a root-mean-square deviation of the points from the fit of 0.03 mag, which is larger than the typical error in $I_{0,RC}$ of ∼0.01 mag. If taken at face value, this represents an age dispersion of ∼1.5 Gyr among the RC stars (based on 0.02 mag/Gyr from the models presented by Sarajedini (1999)).

The mean value of the distance moduli for ten regions is derived to be $(m-M)_{0,RC} = 24.80 \pm 0.04$(random)$\pm 0.05$(systematic) using eq.(6). The errors are derived following the error budget in Table 5. If we use the calibration by Udalski (2000), we obtain $(m-M)_{0,RC} = 24.76 \pm 0.04$(random)$\pm 0.05$(systematic). These values are in excellent agreement with those from the TRGB.

4. DISCUSSION

4.1. *Comparison with Other Studies*

To date the distance to M33 has been studied using a number of standard candles: Cepheid variables (Sandage 1983; Sandage & Carson 1983; Christian & Schommer 1987; Mould 1987; Madore & Freedman 1991; Freedman, Wilson, & Madore 1991; Freedman et al. 2001; Lee et al. 2001), horizontal branch stars in globular clusters (Sarajedini et al. 2000), red supergiant long-period variables (SLPVs)(Pierce, Jurcevic, & Crabtree 2000), the luminosity function of the planetary nebulae (PNLF)(Magrini et al. 2000) and the TRGB (Mould & Kristian 1986; Lee, Freedman, & Madore 1993; Salaris & Cassisi 1998), as summarized in Table 6 (see also van den Bergh (1991),van den Bergh (1999),van den Bergh (2000)). These distance moduli range from as low as 24.41 to a high of 24.85. Our values of 24.80, 24.81 (from the RC with Popowski (2000) calibration and the TRGB) and 24.76 (from the RC with Udalski (2000) calibration) are at the high end of the published range of distances.

Among the previous distance estimates, Lee et al. (2001) determined the distance to M33 using the single phase I-band photometry of 21 Cepheids with $\log P > 0.8$ based on the same data as used in this paper. Lee et al. (2001) obtained $(m-M)_0 = 24.52 \pm 0.13$ for for an adopted total reddening of M33, $E(B-V) = 0.20 \pm 0.04$ ($E(V-I) = 0.27 \pm 0.05$) given by Freedman et al. (2001), the reddening to the LMC, $E(B-V) = 0.10$, and the distance to the LMC, $(m-M)_0 = 18.50$. This value is ∼ 0.3 mag smaller than those derived using the TRGB and RC in this study. This difference is considered partially due to the uncertainty in the estimates of the total reddening for Cepheids in M33. Note that Freedman, Wilson, & Madore (1991) derived the total reddening of M33 Cepheids from $BVRI$ photometry to be $E(B-V) = 0.10 \pm 0.09$, while Freedman et al. (2001) revised this value to $E(B-V) = 0.20 \pm 0.04$ using the different period-luminosity relations for V and I with the same data. Better estimates of the reddening of M33 Cepheids are needed to investigate further this problem.

4.2. *Magnitude difference between the TRGB and the RC*

In the previous section we have examined the dependence on metallicity of the I-band magnitude of the red clump and the magnitude of the TRGB. Here we investigate the dependence on metallicity of both together using the difference of the I-band magnitude between the RC and the TRGB, ΔI(RC–TRGB) = $I_{RC} - I_{TRGB}$. ΔI(RC–TRGB) can be measured directly from the photometry and has the added advantage of being extinction-free (Bersier 2000). Figure 10 displays ΔI(RC–TRGB) versus [Fe/H] for the ten regions in M33. It is seen clearly that there is a positive correlation between ΔI(RC–TRGB) and [Fe/H]. The data for the outer 8 regions in M33 are fit well by ΔI(RC–TRGB)= 0.45[±0.18][Fe/H]+3.95[±0.14]. If we use the data for all regions including the inner two regions, we derive ΔI(RC–TRGB)= 0.56[±0.15][Fe/H]+4.04[±0.11]. The error for the slope is rather large, because the range of [Fe/H] used for this fit is small. Since the TRGB magnitudes and foreground extinctions for all the regions are almost constant, $M_I^{TRGB} = -4.0$ and $A_I = 0.08$ (as given in Table 2), the slope in this fit represents basically the dependence of the RC magnitude on [Fe/H]. The slope derived from the data of M33 is rather steeper than the slope given by Popowski (2000) which is based on the galactic RC stars (shown by the dashed line in Figure 10). For a better determination of the dependence of ΔI(RC–TRGB) on [Fe/H], a large range of [Fe/H] is required.

We have compared ΔI(RC–TRGB) for M33 with those for other nearby galaxies compiled by Bersier (2000) in Figure 11. For M33 the mean difference $< \Delta I >= 3.62 \pm 0.05$ and mean metallicity $< [Fe/H] >= -0.75 \pm 0.07$ of the outer eight regions (excluding R14 and R12) are used from this study. Figure 11 shows that the data for M33 is consistent with those for other galaxies, following the relation plotted in Figure 10.

5. SUMMARY

We present VI photometry of field stars in ten regions located at $R = 2.6$ to 17.8 arcmin from the center of M33 based on $HST/WFPC2$ images. From this photometry we have determined the distance to M33 using the tip of the red giant branch (TRGB) and the red clump (RC). Main results obtained in this study are summarized as follows.

1. Mean metallicities of the RGB in ten regions range from [Fe/H]=–0.9 to –0.6. We find a clear negative radial gradient of the metallicity of the RGB, which has a smaller slope and much smaller scatter than that derived from HII regions in M33.

2. I-band magnitudes of the TRGB in ten regions are almost constant with a very narrow range: $I = 20.82$ to 20.92. This result confirms that the I-band magnitudes of the TRGB is insensitive to age or metallicity for old stars with [Fe/H]< -0.7 (Lee, Freedman, & Madore 1993).

3. The distance to M33 based on the TRGB of ten regions is derived to be $(m-M)_{0,TRGB} = 24.81 \pm 0.04(\text{random})^{+0.15}_{-0.11}$(systematic) (corresponding to a distance of 916 ± 17(random) kpc).

4. Mean colors of the RC in ten regions are almost constant: $(V-I)_0 = 0.89$ to 0.97, and show little correlation with [Fe/H].

5. I-band magnitudes of the RC in ten regions are almost constant with a very narrow range: $I = 24.46$ to 24.57, but they show a correlation with [Fe/H] with a slope similar to that given by Popowski (2000).

6. Assuming the metallicity of the RC stars is the same as that of the RGB stars, the distance to M33 based on the RC of ten regions is derived to be $(m - M)_{0,RC} = 24.80 \pm 0.04(\text{random}) \pm 0.05(\text{systematic})$ (corresponding to a distance of 912 ± 17(random) kpc), which is in excellent agreement with the TRGB distance obtained in this study.

M.G.L. is in part supported by the MOST/KISTEP International Collaboration Research Program (1-99-009). M.G.L. is grateful to the Astronomy Group at the University of Concepcion for the warm hospitality during his stay for this work. A.S. has benefited from financial support from NSF CAREER grant No. AST-0094048. D.G. acknowledges financial support for this project received from CONICYT through Fondecyt grant 8000002.

REFERENCES

Bersier, D. 2000, ApJ, 543, L23
Cannon, R. D. 1970, MNRAS, 150, 111
Cardelli, J. A., Clayton, G. C., & Mathis, J. S. 1989, ApJ, 345, 245
Castellani, V., Degl'Innocenti, S., Girardi, L., Marconi, M., Prada Moroni, P. G., & Weiss, A. 2000, A&A, 354, 150
Christian, C. A., & Schommer, R. A. 1987, AJ, 93, 557
Cioni, M. R., van der Marel, R. P., Loup, C., & Habing, H. J. 2000, A&A, 359, 601
Cole, A. A. 1998, ApJ, 500, L137
Cotton, W. D., Condon, J. J., & Arbizzani, E. 1999, ApJS, 125, 409
Dolphin, A. E. 2000a, PASP, 112, 1383
Dolphin, A. E. 2000b, PASP, 112, 1397
Dolphin, A. E., Saha, A., Skillman, E. D., Tolstoy, E., Cole, A. A., Dohm-Palmer, R. C, Gallagher, J. S., Mateo, M., & Hoessel, J. G. 2001, ApJ, 550, 554
Ferrarese, L., et al. 2000, ApJ, 529, 745
Freedman, W. L., Wilson, C. D., & Madore, B. F. 1991, ApJ, 372, 455
Freedman, W. L., et al. 2001, ApJ, 553, 47
Girardi, L. 2000, Highlights of Astronomy, Vol.12
Girardi, L., Groenewegen, M. A. T., Weiss, A., & Salaris, M. 1998, MNRAS, 301, 149
Girardi, L., & Salaris, M. 2001, MNRAS, 323, 109
Holtzman, J. A., et al. 1995, PASP, 107, 1065
Janes, K. A. 1979, ApJS, 39, 135
King, J. R. 2000, AJ, 120, 1056
Kwitter, K. B., & Aller, L. H., 1981, MNRAS, 195, 939
Lee, M. G. 1996, Jour. Korean Astro. Soc., 29, S67
Lee, M. G., Freedman, W. L., & Madore, B. F. 1993, ApJ, 417, 553
Lee, M. G., Kim, M., Sarajedini, A., Geisler, D., & Gieren, W. 2001, ApJ, submitted
Madore, B. F., & Freedman, W. L. 1991, PASP, 103, 933
Magrini, L., Corradi, R. L. M., Mampaso, A., & Perinotto, M. 2000, A&A, 355, 713
McCall, M. L., Rybski, P. M., & Shields, G. A. 1985, ApJS, 57, 1
Mould, J. 1987, PASP, 99, 1127
Mould, J., & Kristian, J. 1986, ApJ, 305, 591
Paczyński, B., & Stanek, K. Z. 1998, ApJ, 494, L219
Pierce, M. J., Jurcevic, J. S., & Crabtree, D. 2000, MNRAS, 313, 271
Popowski, P. 2000, ApJ, 528, L9
Regan, M. W., & Vogel, S. N. 1994, ApJ, 434, 536
Sakai, S., Zaritsky, D., & Kennicutt, R. C., Jr. 2000, AJ, 119, 1197
Salaris, M., & Cassisi, S. 1998, MNRAS, 298,166
Sandage, A. 1983, AJ, 88, 1108
Sandage, A., & Carlson, G. 1983, ApJ, 267, L25
Sarajedini, A. 1999, AJ, 118, 2321
Sarajedini, A., Geisler, D., Harding, P., & Schommer, R., 1998, ApJ, 508, L37
Sarajedini, A., Geisler, D., Schommer, R., & Harding, P. 2000, AJ, 120, 2437
Saviane, I., Rosenberg, A., Piotto, G., & Aparicio, A. 2000, A&A, 355, 966
Schlegel, D. J., Finkbeiner, D., P., & Davis, M. 1998, ApJ, 500, 525
Stanek, K. Z., & Garnavich, P. M. 1998, ApJ, 503, L131
Stanek, K. Z., Zaritsky, D., & Harris, J., 1998, ApJ, 500, L141
Udalski, A. 1998, Acta Astron., 48, 383
Udalski, A. 2000, ApJ, 531, L25
Udalski, A., Szymański, M., Kubiak, M., Pietrzyński, G., Woźniak, P., & Żebruń, K. 1998, Acta Astron.,48, 1
van den Bergh, S. 1991, PASP, 103, 609
van den Bergh, S. 1999, A&A Rev., 9, 273
van den Bergh, S. 2000, The Galaxies of the Local Group, Cambridge: Cambridge Univ. Press, p.72
Vilchez, J. M., Pagel, B. E. J., Diaz, A. I. , Terlevich, E., & Edmunds, M. G., 1988, MNRAS, 235, 633
Zaritsky, D., Kennicutt, R. C. Jr., & Huchra, J. P. 1994, ApJ, 420, 87
Zaritsky, D., Harris, J., & Thompson, I. 1997, AJ, 114, 1002

TABLE 1
A LIST OF THE REGIONS IN M33 USED FOR ANALYSIS

Region	R.A.(2000) [a]	Dec.(2000) [b]	R[c]	R_{dp}[d]	$E(V-I)$[e]
R14	1 34 0.80	+30 41 3.21	2.55	3.26	0.056
R12	1 34 5.62	+30 38 40.01	3.28	5.84	0.057
U77	1 33 26.70	+30 41 17.72	5.50	9.80	0.056
U49	1 33 47.30	+30 47 54.56	8.34	10.21	0.055
M9	1 34 32.40	+30 38 24.50	8.98	15.67	0.061
H10	1 33 32.68	+30 48 58.39	10.15	14.82	0.055
H38	1 33 49.76	+30 28 57.86	10.65	12.13	0.061
U137	1 33 13.33	+30 28 51.51	13.47	14.32	0.060
C20	1 34 42.54	+30 52 41.41	17.12	18.70	0.062
C38	1 33 28.31	+30 22 28.22	17.83	18.12	0.063

[a]Right ascension in units of hours, minutes, and seconds.

[b]Declination in units of degrees, arcminutes, and arcseconds.

[c]Radial distance in arcminutes from the center of M33.

[d]Deprojected radial distance in arcminutes from the center of M33.

[e]Foreground reddening from COBE/IRAS maps of Schlegel, Finkbeiner, & Davis (1998).

TABLE 2
ESTIMATED PARAMETERS FOR THE TIP OF THE RED GIANT BRANCH METHOD

Region	I_{TRGB}	$I_{0,TRGB}$	$(V-I)_{0,TRGB}$	$(V-I)_{0,-3.5}$	[Fe/H]	$M_{I,TRGB}$	$(m-M)_{0,TRGB}$
R14	20.82 ± 0.05	20.74	2.50 ± 0.06	1.89 ± 0.01	–0.61 ± 0.09	–3.97	24.71
R12	20.87 ± 0.05	20.79	2.35 ± 0.06	1.81 ± 0.01	–0.65 ± 0.09	–4.00	24.79
U77	20.87 ± 0.05	20.79	2.35 ± 0.06	1.76 ± 0.01	–0.68 ± 0.09	–3.99	24.78
U49	20.87 ± 0.05	20.80	2.35 ± 0.05	1.78 ± 0.01	–0.67 ± 0.09	–3.99	24.79
M9	20.92 ± 0.05	20.84	2.05 ± 0.05	1.68 ± 0.02	–0.79 ± 0.10	–4.04	24.88
H10	20.92 ± 0.05	20.84	2.30 ± 0.05	1.73 ± 0.02	–0.71 ± 0.09	–4.00	24.84
H38	20.82 ± 0.05	20.74	2.15 ± 0.05	1.73 ± 0.01	–0.72 ± 0.09	–4.03	24.77
U137	20.87 ± 0.05	20.79	2.25 ± 0.05	1.71 ± 0.02	–0.74 ± 0.09	–4.00	24.79
C20	20.87 ± 0.05	20.78	2.05 ± 0.05	1.66 ± 0.02	–0.82 ± 0.09	–4.04	24.82
C38	20.92 ± 0.05	20.83	2.00 ± 0.05	1.63 ± 0.01	–0.86 ± 0.09	–4.04	24.88

Table 3
ERROR BUDGET FOR THE TRGB METHOD

	Error	Estimation (mag)
1.	Random Error	
	A. Reddening	0.03
	B. Photometry	0.008
	C. Tip detction	0.05
	D. Color spread in the RGB population	0.02
	E. HST photometric calibration	0.12
	F. Total	0.135
	G. Total for 10 regions	0.04[a]
	H. Total for 6 regions	0.06[a]
2.	Systematic Error	
	A. RR Lyrae distance scale	0.11
	B. Undersampling in the Galactic globular cluster calibration[b]	0.1
	C. Total	$^{+0.15}_{-0.11}$

[a] G *or* $H = F/\sqrt{number\ of\ regions}$ which is included the statistical errors.

[b] This error is propagated in only one direction which underestimates the TRGB brightness.

Table 4
ESTIMATED PARAMETERS FOR THE RED CLUMP METHOD

Region	I_{RC}	$I_{0,RC}$	σ_{RC}	$(V-I)_{0,RC}$[a]	$[Fe/H]$[b]	$(m-M)_{0,RC}$[c]	$(m-M)_{0,RC}$[d]
R14	24.57 ± 0.02	24.49	0.33 ± 0.09	0.93 ± 0.006	–0.61 ± 0.09	24.84	24.80
R12	24.52 ± 0.02	24.44	0.41 ± 0.19	0.89 ± 0.006	–0.65 ± 0.09	24.80	24.76
U77	24.49 ± 0.01	24.41	0.38 ± 0.07	0.92 ± 0.004	–0.68 ± 0.09	24.77	24.73
U49	24.52 ± 0.01	24.44	0.34 ± 0.06	0.93 ± 0.004	–0.67 ± 0.09	24.79	24.75
M9	24.49 ± 0.01	24.40	0.24 ± 0.01	0.94 ± 0.004	–0.79 ± 0.09	24.78	24.74
H10	24.56 ± 0.01	24.48	0.26 ± 0.02	0.97 ± 0.004	–0.71 ± 0.09	24.84	24.80
H38	24.53 ± 0.01	24.44	0.25 ± 0.02	0.89 ± 0.004	–0.72 ± 0.09	24.81	24.76
U137	24.53 ± 0.01	24.44	0.25 ± 0.01	0.93 ± 0.004	–0.74 ± 0.09	24.81	24.76
C20	24.46 ± 0.01	24.37	0.21 ± 0.01	0.92 ± 0.004	–0.82 ± 0.09	24.76	24.71
C38	24.49 ± 0.01	24.40	0.21 ± 0.01	0.92 ± 0.003	–0.86 ± 0.09	24.80	24.75

[a] Values from the mean loci of RC with $I_{0,RC}$.

[b] [Fe/H] from the TRGB method. See Table 2.

[c] Distance modulus based on Popowski (2000)'s calibration.

[d] Distance modulus based on Udalski (2000)'s calibration.

TABLE 5
ERROR BUDGET FOR THE RED CLUMP METHOD

	Error	Estimation (mag)
1.	Random error	
	A. Reddening	0.03
	B. Photometry	0.07
	C. Mean I_{RC} detection (fitting error)	0.01
	D. HST photometric calibration	0.12
	E. Total	0.14
	F. Total for 10 regions	0.04[a]
2.	Systematic error	
	A1. calibration error in Powposki (2000)	0.05
	A2. calibration error in Udalski (2000)	0.05

[a] $F = E/\sqrt{number\ of\ regions}$ which includs the statistical error.

TABLE 6
A LIST OF M33 DISTANCE ESTIMATES

Method	$(m-M)_0$	$(m-M)_0$[a]	$E(B-V)$	Reference
Cepheids m_{pg}	24.05 ± 0.18	24.32	0.12	Christian & Schommer (1987)
Cepheids I	24.82 ± 0.15	24.93	0.12	Mould (1987)
Cepheids BVRI	24.64 ± 0.09	24.75	0.10	Freedman, Wilson, & Madore (1991)
Cepheids VI	24.56 ± 0.10	24.87	0.20	Freedman et al. (2001)
Cepheids VI	24.52 ± 0.15	24.83	0.20	Lee et al. (2001)
TRGB	24.70 ± 0.10	24.82	0.10	Mould & Kristian (1986),Lee, Freedman, & Madore (1993)
SLPV	24.85 ± 0.13	24.97	0.10	Pierce, Jurcevic, & Crabtree(2000)
PNLF	24.62 ± 0.25	24.74	0.10	Magrini et al. (2000)
HB	24.84 ± 0.16	—	0.04[b]	Sarajedini et al. (2000)
TRGB	24.81 ± 0.13	—	0.04[b]	This study
RC	24.80 ± 0.14[c]	—	0.04[b]	This study
RC	24.76 ± 0.14[d]	—	0.04[b]	This study

[a]Distance modulus for $E(B-V) = 0.04$.

[b]The foreground reddening value of Schlegel, Finkbeiner, & Davis (1998).

[c]Based on Popowski (2000)'s calibration.

[d]Based on Udalski (2000)'s calibration.

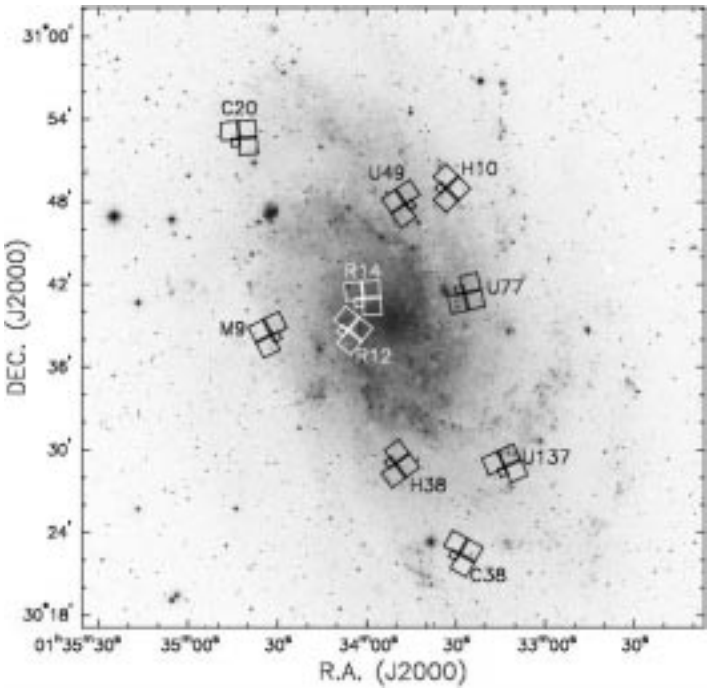

FIG. 1.— A finding chart of M33 showing the positions of the ten regions observed with $HST/WFPC2$ (squares). The grayscale map is from the digitized Palomar Sky Survey.

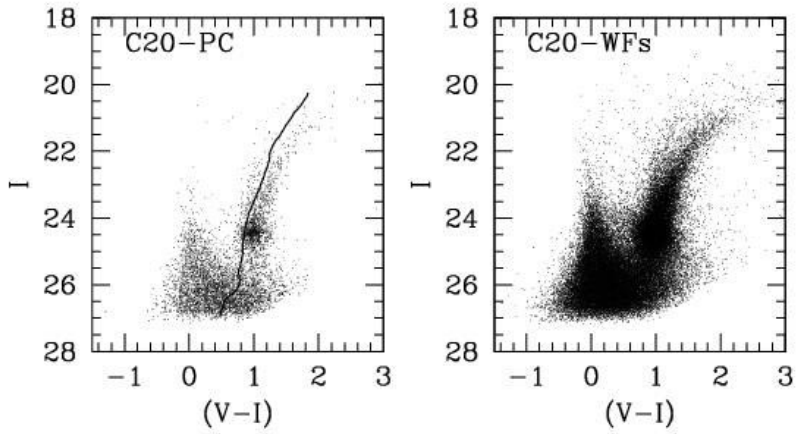

FIG. 2.— Color-magnitude diagrams of the field stars in the PC chip (left panel) and in the WF2, WF3, and WF4 chips (right panel) of the C20-region. The solid line in the left panel represents the mean locus of the globular cluster C20. Note that the mean color of the RGB of the field stars is redder than that of the globular cluster. A compact red clump is found to be at $I \approx 24.4$ and at $(V-I) \approx 0.9$, and the TRGB is seen at $I \approx 21.0$.

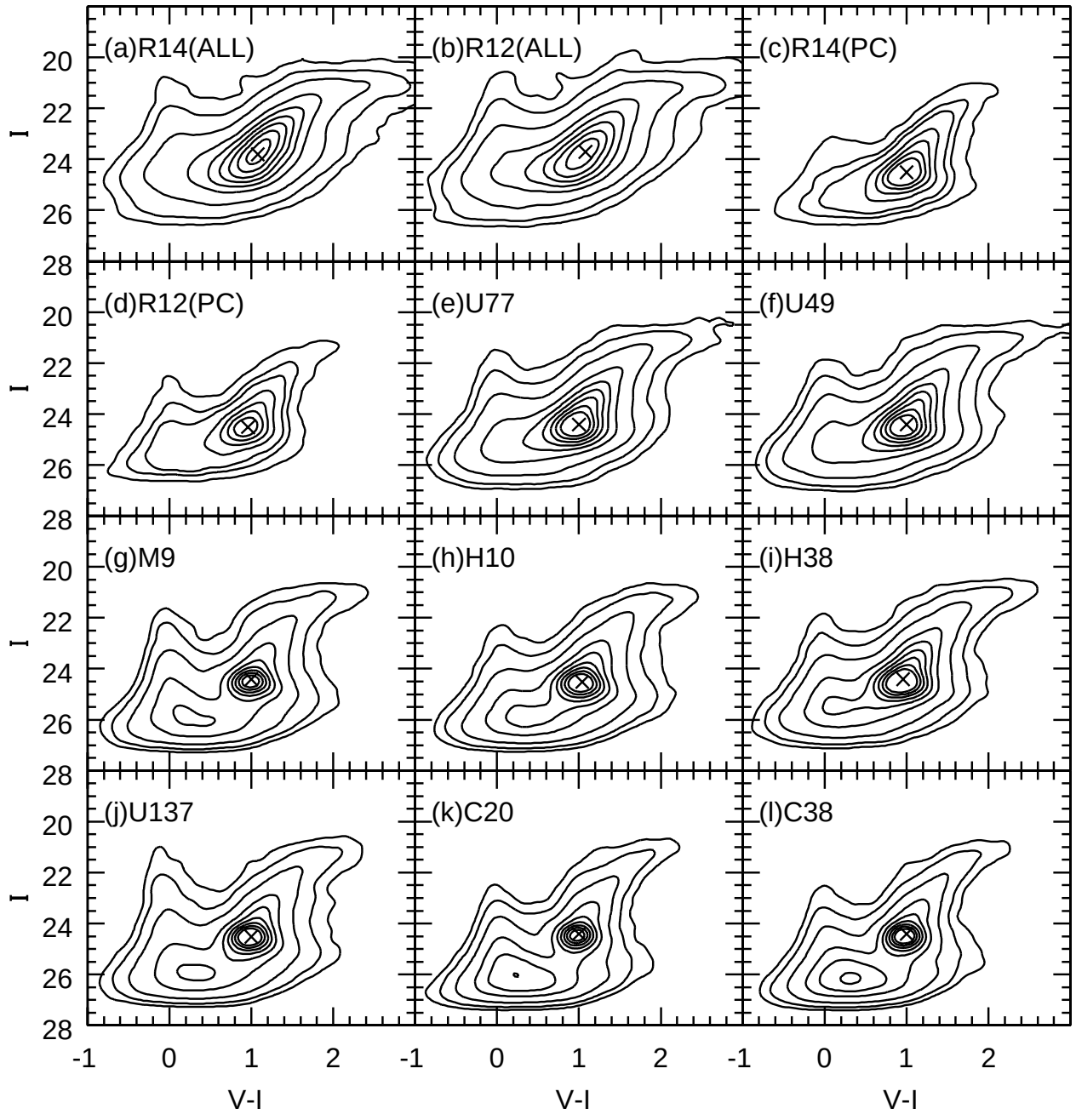

FIG. 3.— Color-magnitude diagrams of the observed regions in M33 displayed in the density contour map. The panels (c) and (d), for R14 and R12 regions, are only for the stars in the PC chip. In other panels the CMDs of the field stars in all four chips (PC, WF2, WF3, and WF4) are displayed. Crosses represent the peaks of the density contour map, which correspond to the mean position of the red clumps. Contour levels are at 1, 3, 10, 30, 50, 70, 90, 110, and 130 stars/grid, respectively. For (c) and (d) contour levels are at 1, 3, 5, 10, 15, 20, and 25 stars/grid, respectively.

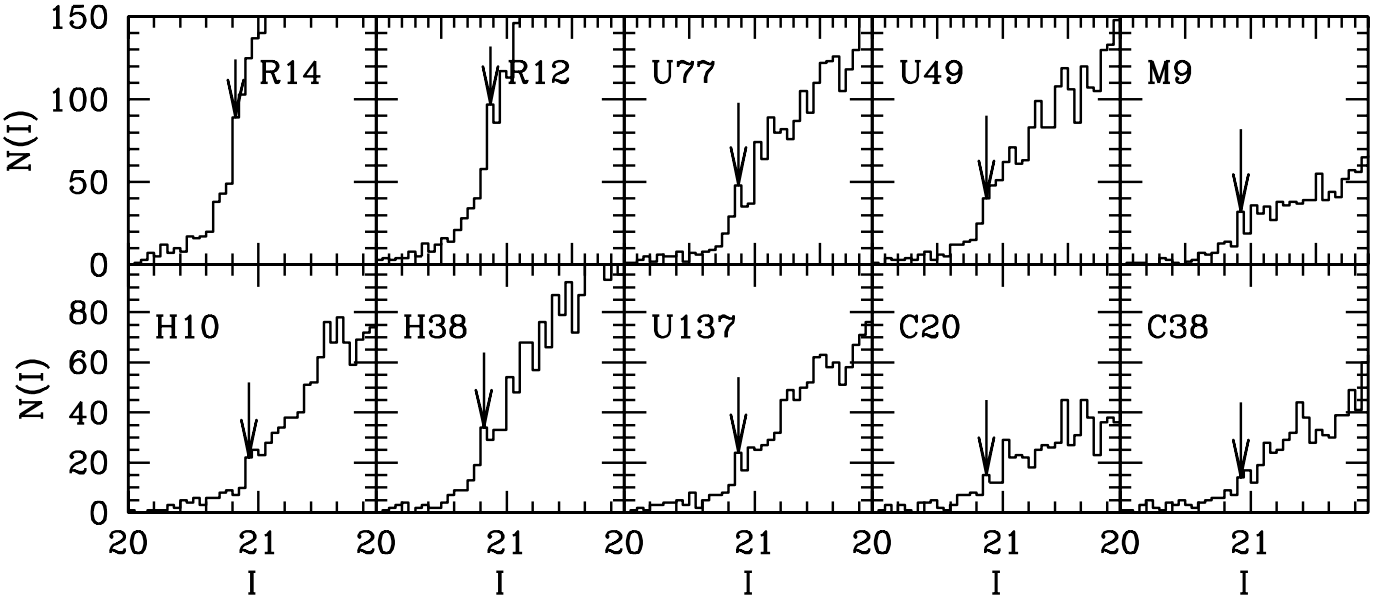

FIG. 4.— I-band luminosity functions of bright red stars in M33. The I magnitudes of the tip of the red giant branch are marked by arrows.

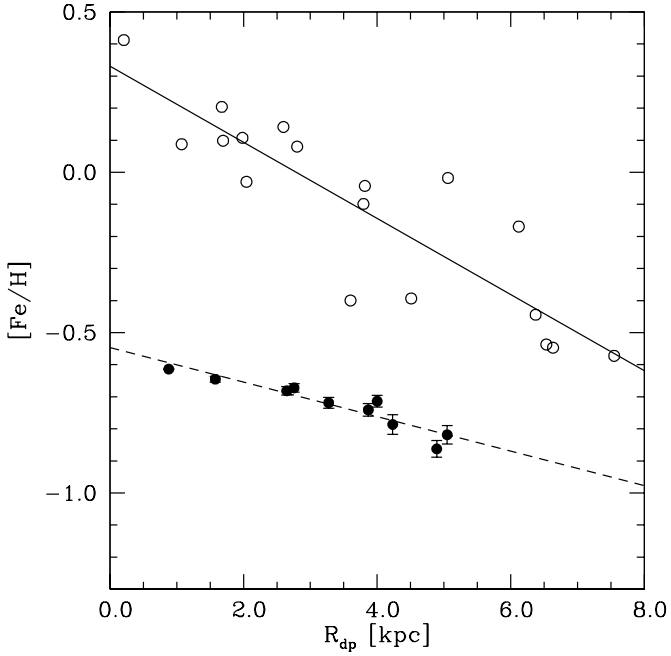

FIG. 5.— Mean metallicity [Fe/H] of the RGB in each region as a function of the deprojected radial distance derived in this study (filled circles). The dashed line represents the mean relation between R_{dp} and [Fe/H] derived from the RGB. The mean metallicity decreases as the radial distance increases. For comparison, the solid line represents the mean relation between R_{dp} and [Fe/H] derived for the HII regions in M33 from various other studies (open circles).

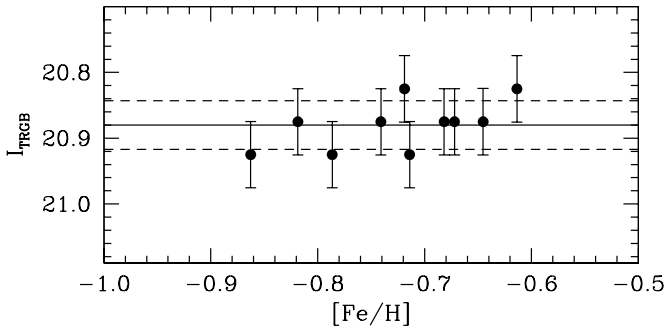

FIG. 6.— The I-band magnitude of the TRGB, I_{TRGB}, as a function of metallicity. The solid line represents the average value of I_{TRGB}, and the dashed lines represent standard deviations of $\pm 1\sigma$.

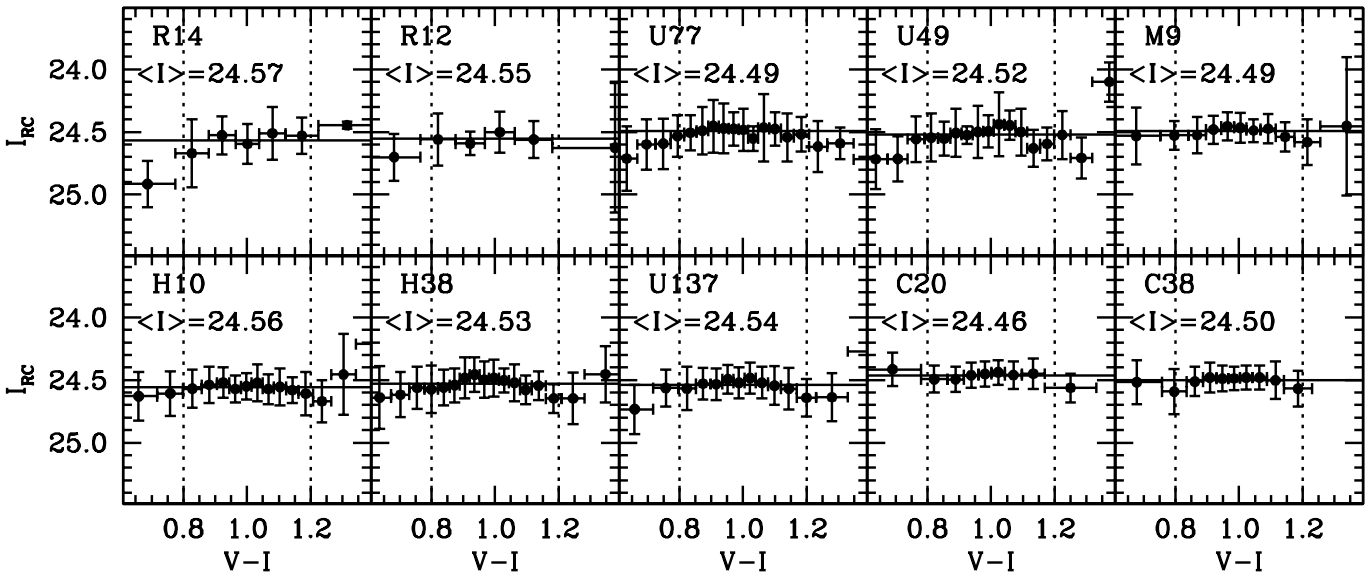

FIG. 7.— The mean magnitude of the red clump I_{RC} versus $(V-I)$ color. The horizontal bars on filled circles represent the sizes of color bins, not error bars, while the vertical bars represent fitting errors. Two thousand stars are included in each color bin. Note that I_{RC} varies little in the color range of $0.8 \leq (V-I) \leq 1.2$ (between the two vertical dotted lines). The horizontal solid line represents the mean of I_{RC} for all color bins.

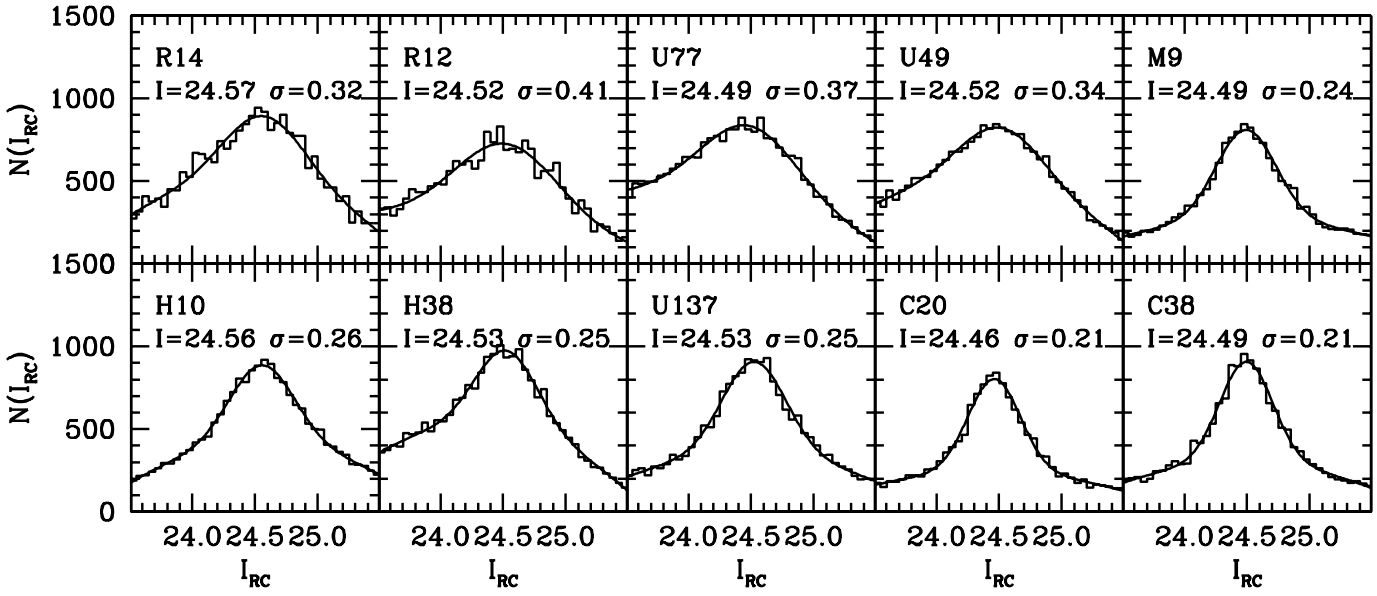

FIG. 8.— I-band luminosity functions of red clump stars in the color range $0.8 < (V-I) < 1.2$ and in the magnitude range $23.5 < I < 25.5$. The solid line is a fitting line with equation (5) as described in the text. The mean magnitude of the red clump I and the dispersion of I, σ, are also shown. The luminosity functions of R14 and R12 regions, in which the stars in only PC chips are used, are multiplied by a factor of 5 arbitrarily.

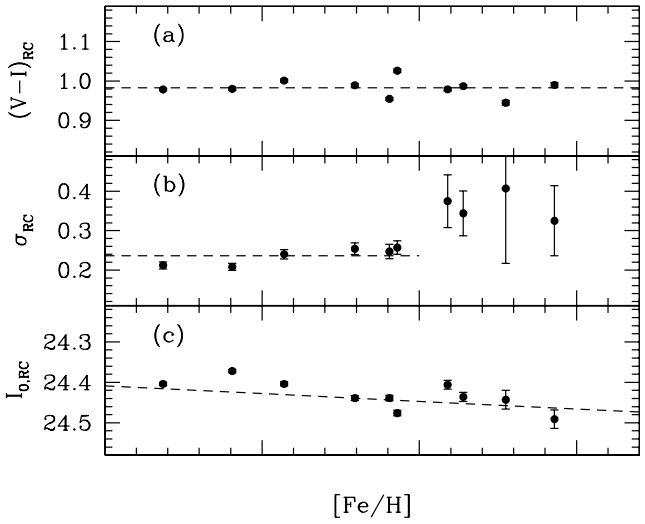

FIG. 9.— Several parameters for the red clump method as a function of metallicity [Fe/H]. (a) The mean color of the red clump $(V-I)_{RC}$. The dashed line represents a mean value of the ten regions. (b) The dispersion of the mean magnitude of red clump. The dashed line represents a mean value of the outer six regions with lower [Fe/H]. (c) The extinction corrected I-band magnitudes of the red clump. The dashed line shows the Popowski (2000)'s calibration for a distance modulus of $(m-M)_0 = 24.81$.

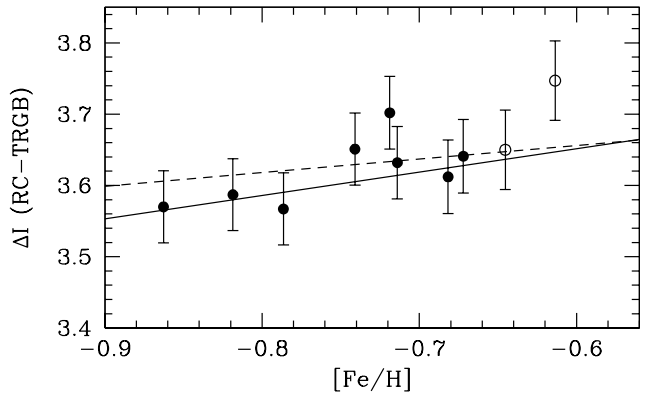

FIG. 10.— The difference in I-band magnitude between the RC and the TRGB, ΔI(RC–TRGB), versus mean metallicity of the red giants in M33. The dashed line represents the expected difference, when the TRGB magnitude $M_I^{TRGB} = -4.0$ and Popowski (2000)'s calibration are assumed. The solid line represents a fitting line to the data when R14 and R12 regions (open circles) are excluded.

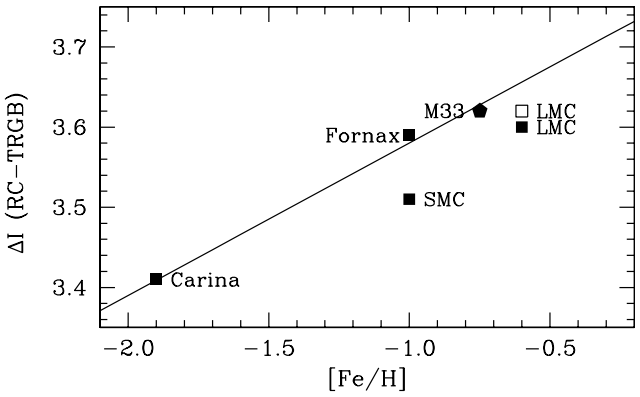

FIG. 11.— The difference in I magnitude between the RC and the TRGB stars ΔI(RC–TRGB) versus metallicity for M33 and other nearby galaxies. A filled pentagon represents our mean value of the eight regions in M33. The LMC data are from Zaritsky, Harris, & Thompson (1997) (open square) and Sakai, Zaritsky, & Kennicutt (2000) (filled square). The solid line represents the expected difference when the TRGB magnitude $M_I^{TRGB} = -4.0$ and Popowski (2000)'s calibration are assumed.